International Journal of Heat and Mass Transfer 53 (2010) 2897–2907

Contents lists available at ScienceDirect

International Journal of Heat and Mass Transfer

journal homepage: www.elsevier.com/locate/ijhmt

# The influence of the non-resolved scales of thermal radiation in large eddy simulation of turbulent flows: A fundamental study

Maxime Roger, Pedro J. Coelho *, Carlos B. da Silva

*Mechanical Engineering Department, Instituto Superior Técnico/IDMEC, Technical University of Lisbon, Av. Rovisco Pais, 1049-001 Lisboa, Portugal*

ARTICLE INFO

*Article history:*
Received 3 April 2009
Accepted 20 January 2010
Available online 1 March 2010

*Keywords:*
Turbulence–radiation interaction (TRI)
Large eddy simulation (LES)
Radiative heat transfer
Direct numerical simulation (DNS)
Subgrid-scale modelling
Homogeneous isotropic turbulence

ABSTRACT

The filtered radiative transfer equation has been solved without subgrid-scale model and compared to a-priori estimations from direct numerical simulation of statistically stationary homogeneous isotropic turbulence. The importance of the large eddy simulation non-resolved scales on the thermal radiation is analysed in this academic case. The influence of the mean and variance of temperature of the system on the subgrid-scale correlations is studied. It is shown that the turbulence–radiation interaction (TRI) is greater for low-temperature flows, where the radiative transfer is lower. Moreover, the strongest subgrid-scale correlations, which are the temperature self-correlation and the absorption coefficient-temperature correlation, have opposite effects, which suggests that it is better to neglect both correlations, instead of modelling only one. Therefore, the assumption of neglecting the TRI in LES leads to good predictions. Three-dimensional filtering effects, as well as the grid influence on non-local quantities, such as the radiation intensity, are also analysed. These effects have a local influence, but are negligible in the tested cases.



## 1. Introduction

Radiative transfer plays a significant role in turbulent reactive flows, and turbulence–radiation interaction (TRI) effects are relevant in most cases [1]. The TRI has generally been investigated using Reynolds-averaged Navier-Stokes (RANS) methods [2], probability density function approaches [3,4] and recently Direct Numerical Simulation (DNS) [5–7]. Although DNS is a powerful tool to provide fundamental insight on turbulent flows [8], it is too computational expensive for practical applications, and is restricted to moderate Reynolds numbers and/or simple geometries. In this context, and with the increase of computer power, large eddy simulation (LES) is becoming an attractive approach to achieve high accuracy at an affordable computational cost for solving moderately complex problems of practical usefulness in the Computational Fluid Dynamics and combustion communities [9].

To the authors' knowledge, few work has been done so far to simulate the TRI in LES of reactive flows. Poitou et al. [10] have made an a-priori study from DNS of a reactive shear layer to evaluate the TRI from the emission part of radiation and have tested models based on Taylor development to reconstruct the correlation between the temperature and the absorption coefficient in a flame. Recently, Coelho [11] investigated the relevance of the TRI in Sandia flame D in the LES framework. He used a stochastic model to generate a time-series of turbulent scalar fluctuations along optical paths of the flame and solved the filtered radiative transfer equation (RTE) along these paths by applying a one-dimensional filtering operation. In this study, various approximations based on an assumed subgrid-scale probability density function are tested to model the subgrid-scale fluctuations of thermal radiation. It is shown that the relevance of the TRI in LES framework is smaller than in RANS calculations, and consequently an extension of the optical thin fluctuation approximation should be a judicious choice in LES. In the studied flame, the average relative error of the filtered radiative intensity is below 0.3%.

Thermal radiation has been coupled to LES of combustion systems in [12–15]. In these studies, the filtered radiation quantities have been estimated without subgrid-scale (SGS) models, i.e., the TRI effects have been simply neglected. The present study is a continuation of previous works [16,17] where the filtered RTE was studied. A conclusion of these works was that neglecting the subgrid-scale influence on the thermal radiation is a good assumption under various physical conditions, e.g., when the turbulence intensity is below 20%, when the medium is not optically thick, and if the filter size remains in the low-inertial range of the kinetic energy spectrum. These conclusions have been drawn from a-priori estimations from DNS (or filtered DNS) of homogeneous isotropic turbulence. However, the filtered RTE was not solved in these studies.

The present study reports an evaluation of the assumption used in [12–15], that consists in neglecting the influence of the unre-

* Corresponding author. Tel.: +351 21 841 81 94; fax: +351 21 847 55 45.
*E-mail addresses:* roger.maxime@ist.utl.pt (M. Roger), pedro.coelho@ist.utl.pt (P.J. Coelho), carlos.silva@ist.utl.pt (C.B. da Silva).

0017-9310/$ - see front matter © 2010 Elsevier Ltd. All rights reserved.
doi:10.1016/j.ijheatmasstransfer.2010.02.002

solved scales over the resolved-scale radiative heat transfer. For this goal, LES without any SGS model of thermal radiation has been carried out, i.e., the filtered RTE has been solved without accounting for the subgrid-scales influence on the radiative quantities. The results obtained have been compared to the reference DNS calculations, and to a-priori estimations in order to analyse the role of the unresolved scales (or SGS) of motion. The influence of the subgrid-scale correlations is identified and analysed, as well as the effect of the three-dimensional filtering and the grid influence, in order to shed some light about a SGS modelling for thermal radiation. These two last issues were not previously investigated, while the first one was not studied in the framework of LES, taking DNS as reference.

The radiative heat transfer has been calculated by using a ray-tracing/correlated *k*-distribution method. The simplest possible turbulent flow configuration, statistically steady (forced) homogeneous isotropic turbulence without combustion, has been chosen in order to give fundamental insight about TRI.

This article is organized as follows. In the next section, the filtered RTE is described, and the hypothesis involved by neglecting the SGS influence in radiative heat transfer are presented. In Section 3, the numerical tools for turbulence and radiation calculations are detailed. In Section 4, the results are presented and discussed. Finally, the article ends with an overview of the main results and conclusions.

## 2. The filtered radiative transfer equation

### 2.1. The filtered radiative intensity

The RTE in the case of an emitting-absorbing and non-scattering medium may be written as [18]:

$$\frac{dI_\nu}{ds} = -\kappa_\nu I_\nu + \kappa_\nu I_{b\nu} \tag{1}$$

where $\nu$ is the wavenumber, $I_\nu$ the spectral radiation intensity, $s$ the coordinate along the optical path, $\kappa_\nu$ the spectral absorption coefficient and $I_{b\nu}$ the Planck function. In LES, the large turbulent motions are directly represented whereas the effect of the small scale motions is modelled [8]. A low-pass filtering operation is performed so that the resulting filtered quantity can be adequately resolved on a coarser grid. Thus, any given flow variable $Q$ can be decomposed into a grid-scale part $\overline{Q}$, and a subgrid-scale part $Q''$: $Q = \overline{Q} + Q''$. The filtered RTE is obtained by applying the spatial filtering operation to the RTE:

$$\begin{aligned}\frac{d\bar{I}_\nu}{ds} &= -\overline{\kappa_\nu I_\nu} + \overline{\kappa_\nu I_{b\nu}} \\ &= -\bar{\kappa}_\nu \bar{I}_\nu - \left(\overline{\kappa_\nu I_\nu} - \bar{\kappa}_\nu \bar{I}_\nu\right) + \bar{\kappa}_\nu \bar{I}_{b\nu} + \left(\overline{\kappa_\nu I_{b\nu}} - \bar{\kappa}_\nu \bar{I}_{b\nu}\right)\end{aligned} \tag{2}$$

The terms in parentheses, $\left(\overline{\kappa_\nu I_\nu} - \bar{\kappa}_\nu \bar{I}_\nu\right)$ and $\left(\overline{\kappa_\nu I_{b\nu}} - \bar{\kappa}_\nu \bar{I}_{b\nu}\right)$, need to be modelled in order to close the filtered RTE. They represent the effects of the unresolved scales on the monochromatic radiative intensity.

The simplest way to close Eq. (2) is to suppose that the subgrid-scale fluctuations of thermal radiation are negligible, i.e., the terms $\left(\overline{\kappa_\nu I_\nu} - \bar{\kappa}_\nu \bar{I}_\nu\right)$ and $\left(\overline{\kappa_\nu I_{b\nu}} - \bar{\kappa}_\nu \bar{I}_{b\nu}\right)$ are neglected in the filtered RTE. In this assumption, the filtered RTE may be written as

$$\frac{d\bar{I}_\nu}{ds} \simeq -\bar{\kappa}_\nu \bar{I}_\nu + \bar{\kappa}_\nu \bar{I}_{b\nu} \tag{3}$$

In the case of a medium composed by a mixture of $H_2O$ and $CO_2$, it is further assumed that $\bar{I}_{b\nu} \simeq I_{b\nu}(\overline{T})$ and $\bar{\kappa}_\nu \simeq \kappa_\nu(\overline{T}, \overline{X}_{CO_2}, \overline{X}_{H_2O})$, i.e., the temperature self-correlation is neglected as well as the correlation between the absorption coefficient and the temperature/chemical composition.

In this study, we have focused on radiative quantities integrated over the spectrum, such as the Planck-mean absorption coefficient $\kappa_P$ and the incident mean absorption coefficient $\kappa_G$, which are defined as follows

$$\kappa_P = \frac{\int_0^{+\infty} \kappa_\nu I_{b\nu} d\nu}{\int_0^{+\infty} I_{b\nu} d\nu} \tag{4}$$

$$\kappa_G = \frac{\int_0^{+\infty} \kappa_\nu G_\nu d\nu}{\int_0^{+\infty} G_\nu d\nu} = \frac{\int_0^{+\infty} \kappa_\nu I_\nu d\nu}{\int_0^{+\infty} I_\nu d\nu} \tag{5}$$

where $G_\nu$ is the spectral incident radiation. The second equality in Eq. (5) only holds for isotropic radiation, as in the present analysis. In this case, the equation for the total filtered intensity may be written as:

$$\frac{d\bar{I}}{ds} = -\overline{\kappa_G I} + \overline{\kappa_P I_b} = -\bar{\kappa}_G \bar{I} - \left(\overline{\kappa_G I} - \bar{\kappa}_G \bar{I}\right) + \bar{\kappa}_P \bar{I}_b + \left(\overline{\kappa_P I_b} - \bar{\kappa}_P \bar{I}_b\right) \tag{6}$$

The assumption of isotropic radiation simplifies the physical problem presented in the remainder of this study. In practical problems, this assumption is approximately valid for perfectly stirred reactors. Furthermore, Eq. (6) is similar to Eq. (2), which does not require the assumption of isotropic radiation, and therefore it is expected that the conclusions drawn from the analysis of Eq. (6) remain valid for Eq. (2).

### 2.2. The filtered divergence of the radiative flux

The divergence of the radiative heat flux may be expressed as [18]:

$$\nabla \cdot \mathbf{q} = \int_0^{+\infty} \kappa_\nu (4\pi I_{b\nu} - G_\nu) d\nu \tag{7}$$

Assuming isotropic radiation, we can rewrite the divergence of the radiative heat flux in the following form

$$\nabla \cdot \mathbf{q} = 4\pi[\kappa_P I_b - \kappa_G I] \tag{8}$$

Applying the filtering operation to Eq. (8) yields

$$\begin{aligned}\overline{\nabla \cdot \mathbf{q}} &= 4\pi\left[\overline{\kappa_P I_b} - \overline{\kappa_G I}\right] \\ &= 4\pi\left[\bar{\kappa}_P \bar{I}_b + \left(\overline{\kappa_P I_b} - \bar{\kappa}_P \bar{I}_b\right) - \bar{\kappa}_G \bar{I} - \left(\overline{\kappa_G I} - \bar{\kappa}_G \bar{I}\right)\right]\end{aligned} \tag{9}$$

and in the case where subgrid-scale fluctuations are neglected:

$$\overline{\nabla \cdot \mathbf{q}} \simeq 4\pi\left[\bar{\kappa}_P \bar{I}_b - \bar{\kappa}_G \bar{I}\right] \tag{10}$$

$$\simeq 4\pi\left[\kappa_P(\overline{T}, \overline{X}_{CO_2}, \overline{X}_{H_2O}) I_b(\overline{T}) - \bar{\kappa}_G \bar{I}_{LES}\right] \tag{11}$$

where the filtered absorption $\bar{\kappa}_G \bar{I}_{LES}$ is given by the resolution of Eq. (3) and from Eq. (5). In Eq. (6) or (9), the terms depending on $\kappa_P$ and $I_b$ will be referred to as the emission terms and those depending on $\kappa_G$ and $I$ as the absorption terms of the filtered RTE.

## 3. Computational details

In this section, the method used to solve the filtered RTE is described as well as the procedure employed to obtain the a-priori results. Both procedures have as a starting point the instantaneous fields of a passive scalar obtained from DNS of statistically stationary (forced) homogeneous isotropic turbulence. In Section 3.1, the DNS calculations are detailed and it is explained how the passive scalar field is used to define the temperature and the chemical composition of the medium. The DNS and the radiative transfer calculations are decoupled. Although radiation from $H_2O$ could easily be included in the calculations, only radiation from carbon dioxide is considered here in order to reduce computational requirements. This is sufficient for our main goal in this paper, namely to investigate the TRI in the context of LES.

For the LES, a spatial filtering operation is applied to the temperature and to the species concentration fields. The new coarser

grid used in the LES is defined according to the filter size, as described in Section 3.2. In Section 3.3, the ray-tracing/correlated $k$-distribution method used to solve the filtered RTE is presented. Finally Section 3.4 presents a brief description of the methodology used to obtain the filtered DNS results, which will be used as reference in Section 4.

### 3.1. Direct numerical simulation of homogeneous isotropic turbulence

In the present work, the Navier-Stokes equations are solved for an incompressible, constant property flow. A simple transport equation is also solved along with the Navier-Stokes equations to determine the evolution of a passive scalar field. The equations are numerically integrated with direct numerical simulation (DNS). The DNS is carried out using a standard pseudo-spectral scheme for spatial discretization, and the temporal advancement is made with an explicit 3*rd* order Runge-Kutta scheme. The passive scalar field has a Schmidt number equal to 0.7. The physical domain is a cubic box of size $2\pi$. The simulations use $192^3$ collocation points, and were fully dealised using the 3/2 rule.

The large scales of both the velocity and the scalar fields were forced in order to sustain the turbulence, using the method described in [19]. The forcing was imposed on three wave numbers concentrated on $k_p = 3$ for the velocity and the scalar field. It consists in injecting kinetic energy and scalar variance during the simulation at a rate that approximately balances the instantaneous viscous and passive scalar dissipation rates. After an initial transient at the start of the simulation, both the velocity and passive scalar fields reach a statistically stationary state. The forcing affects only a very small wave number region associated with the large scales of motion, and not the inertial range region that is used in the a-priori tests.

Table 1 lists some of the flow parameters, namely the Reynolds number based on the Taylor micro-scale, $Re_\lambda$, the velocity integral length scale, $L_{11}$, and the Kolmogorov micro-scale, $\eta$. The molecular viscosity is $\nu$ and the maximum resolved wave number is $k_{max}$. The skewness $S$ and flatness $F$ factors of the velocity derivative are similar to the ones found in high Reynolds number turbulence. Moreover, the energy and scalar variance spectra (not shown) exhibit an inertial range with about one decade, and furthermore the Reynolds number based on the Taylor micro-scale is close to 100. These results show that at least the inertial and dissipative ranges of scales of motion from the present simulation are characteristic of the flow in mixing layers, jets, and wakes, at the far field and at moderate Reynolds numbers. More details on this DNS data bank can be found in [20,21].

The data obtained from homogeneous isotropic turbulence simulations in the cubic box are rescaled into the radiation domain by assuming kinematics similarity between the two flows [17,20]. This assumption yields the following expression of the instantaneous temperature field $T$ used in the radiative heat transfer calculations as a function of the DNS temperature field $T_{DNS}$

$$T(\mathbf{x}) = \langle T\rangle + T_{DNS}(\mathbf{x})\sqrt{\frac{\langle T'^2\rangle}{\langle T'^2_{DNS}\rangle}} \tag{12}$$

Here, $\langle T\rangle$ is the time-averaged temperature, and $\langle T'^2\rangle$ and $\langle T'^2_{DNS}\rangle$ are the variance of the temperature fields prescribed for the radiation calculations and computed from DNS, respectively. A similar procedure is used to rescale the instantaneous species concentration field of the absorbing species. This rescaling from DNS data to radiation calculations should be manipulated carefully, especially in cases where the fluctuation intensities are large. At some points, the temperature is beyond the physical range. In those cases, we may assume that $T(\mathbf{x}_i) = T_{\max}$ in points where the temperature exceeds the maximum possible temperature of the system, which is assumed to be $T_{\max} = 2500$ K (and the same for points $\mathbf{x}_j$ where $T(\mathbf{x}_j)$ is lower than $T_{\min} = 300$ K). This assumption remains acceptable as long as the statistics of the temperature field are not significantly modified, which is the case if the temperature turbulence intensity, defined by $\sqrt{\langle T'^2\rangle}/\langle T\rangle$, does not exceed 30% for $\langle T\rangle = 1500$ K [17]. In the case where $\sqrt{\langle T'^2\rangle}/\langle T\rangle = 20\%$, the mean temperature $\langle T\rangle$ (in K) may belong to the interval $1000 \leqslant \langle T\rangle \leqslant 1800$.

**Table 1**
Physical and computational parameters of the DNS of isotropic turbulence.

| $Re_\lambda$ | $\nu$ | $Sc$ | $k_{max}\eta$ | $L_{11}$ | $\eta$ | $S$ | $F$ |
|---|---|---|---|---|---|---|---|
| 95.6 | 0.006 | 0.7 | 1.8 | 1.24 | $2.8\times10^{-2}$ | −0.49 | 4.63 |

### 3.2. LES without SGS of thermal radiation

To calculate the radiative transfer quantities in LES framework, a filtering operation is applied to the temperature and the species concentration fields. In this study, we are interested in analyzing those features of the radiative heat transfer that are relevant in the physical space, i.e. LES using finite difference or finite volume codes, since this procedure is more often used in LES of turbulent flows for engineering applications. Therefore, the box filtering operation has been chosen, since this filter type is implicitly associated with the discretization using central differences or finite volume codes [22]. The box filter function is defined such that $\overline{Q}$ represents the quantity $Q$ averaged over a cell of volume $\Delta^3$ (where $\Delta$ is the filter size) :

$$\overline{Q} = \frac{1}{\Delta^3}\int\int\int_{\Delta^3} Q(\mathbf{x},t)d\mathbf{x} \tag{13}$$

The temperature $T$ and the $CO_2$ molar concentration $X_{CO_2}$, obtained from DNS, are filtered using Eq. (13) in order to obtain $\overline{T}$ and $\overline{X}_{CO_2}$. After this, the filtered quantities are used as input in the radiative transfer calculations described in Section 3.3. Five different filter sizes were used with $\Delta = m\delta$, where $m = 2, 4, 8, 16$ and 32 ($\delta$ is the mesh size in the DNS grid). The filtered radiation quantities were estimated in two different grids, namely the initial DNS grid (with a control volume of size $\delta^3$) and a coarser grid with a control volume equal to $\Delta^3$, like it is usually done in LES.

In practice, LES should be carried out using $\Delta/\delta = 8$ or 16 which correspond to the filter sizes located at the inertial range region of the kinetic energy spectrum in the present simulations [21]. In the following, the results obtained with the filter size $\Delta/\delta = 16$ are emphasized because they are more representative of the implicit filter sizes used in practical engineering applications [21].

### 3.3. Radiative transfer calculations

The ray-tracing method is used for the radiation calculations. It consists in solving the RTE, along a line of sight, in its integral form, which may be written as [18]

$$I_\nu(s) = I_\nu(0)\exp\left(-\int_0^s \kappa_\nu(s')ds'\right) + \int_0^s \kappa_\nu(s')I_{b\nu}(s') \times \exp\left(-\int_{s'}^s \kappa_\nu(s'')ds''\right)ds' \tag{14}$$

Eq. (14) has been discretized by dividing the optical paths into elements and interpolating the temperature and chemical composition using cubic splines. This interpolation is used to compute the integrals in Eq. (14), which are numerically evaluated using Simpson's rule, to guarantee that the order of accuracy in the evaluation of the radiation intensity is similar to that of DNS. When the LES with-

out SGS models is carried out, the interpolations are applied on the filtered temperature and on the filtered chemical composition fields, whereas when DNS or filtered DNS are considered, this interpolation is applied on the $T$ and $X_{CO_2}$ fields.

Periodic boundary conditions were employed in the present work to be consistent with the boundary conditions used in the isotropic DNS. These conditions have also been used in the study of Deshmukh et al. [6] and in [17]. The periodicity was enforced by setting $I_\nu(L) = I_\nu(0)$ where $L$ is the length of the radiation domain. Physically, the periodic conditions imply that the medium is in radiative equilibrium. As long as the optical thickness is not small (like in the cases discussed in the following), these boundary conditions have no significant effect on the thermal radiation subgrid-scale fluctuations.

The integration over the spectrum has been done using the correlated-k distribution method (CK approximation) [23]. In this method, the spectrum is divided into narrow bands such that $\int_0^{+\infty} I_\nu d\nu \simeq \sum_{i=1}^{N_b} I_{\Delta\nu_i}$, and the absorption coefficient is reordered within every band into a smooth monotonically increasing function. The averaged radiation intensity over a band takes the following form

$$I_{\Delta\nu} = \frac{1}{\Delta\nu}\int_{\Delta\nu} I_\nu d\nu = \int_0^{+\infty} I(k)f(k)dk = \int_0^1 I(g)dg \tag{15}$$

where $f(k)$ is the probability density function of the absorption coefficient in the considered band and $g(k)$ is the cumulative $k$-distribution function. The integral in Eq. (15) is evaluated using a Gaussian quadrature, which yields the following relation for a medium with one absorbing species

$$I_{\Delta\nu} = \sum_{i=1}^{N_b}\sum_{j=1}^{N_Q} \omega_j I_{\Delta\nu_i j}\Delta\nu_i \tag{16}$$

where $\omega_j$ is the quadrature weight, $N_Q$ is the number of quadrature points, and $I_{\Delta\nu_i j}$ is the radiative intensity for the $i$th band and for the quadrature point $j$. The parameters needed for the CK approximation are taken from the data of Soufiani and Taine [24]. It was assumed that the temperature and the absorbing species are fully correlated, which is consistent with the laminar flamelet combustion model.

### 3.4. A-priori calculation of thermal radiation

The procedure used to obtain the a-priori results from the filtered DNS is the same as the one described in [17]. The radiative transfer equation is solved by the ray-tracing/CK method and the radiative quantities such as the intensity $I$, the absorption $\kappa_G I$ or the emission $\kappa_P I_b$, are then filtered according to Eq. (13) using a box filter of size $\Delta = m\delta$, with $m = \{2, 4, 8, 16, 32\}$. In this way, it is possible to obtain all the filtered quantities (like for instance, concerning the radiative emission, $\overline{\kappa_P I_{bDNS}}$ or $\bar{\kappa}_P \bar{I}_{bDNS}$), which will serve as a reference for the study of the role of various subgrid-scale correlations (see Section 4).

## 4. Results and discussion

In this section, the results obtained from LES without subgrid-scale model are compared to the DNS and to the a-priori (or filtered DNS) results. In the remainder of the paper, it is implicit that LES refers to LES without subgrid-scale model.

The standard radiative transfer calculations were carried out assuming that the mean temperature of the medium is 1500 K and the mean molar fraction of $CO_2$ is 0.5. The root mean square (rms) of temperature and carbon dioxide molar fraction are 300 K and 0.1, respectively. These values of the rms correspond to a temperature turbulence intensity, defined by $\sqrt{\langle T'^2\rangle}/\langle T\rangle$, equal to 20%. The length $L$ of the radiation domain is defined in order to satisfy the prescribed optical thickness of the medium $\tau$, estimated from $\tau = \kappa_P(\langle T\rangle, \langle X_{CO_2}\rangle)L$, and which is set equal to 10. In the following calculations, these standard values remain unchanged unless other values are indicated.

An example of instantaneous radiation intensity fields is presented in Fig. 1. Fig. 1(a) displays the field calculated from DNS, whereas Fig. 1(b) and (c) display the fields obtained from filtered DNS in the DNS grid and in the coarse LES grid, respectively. The fields calculated from LES are presented in Fig. 1(d) (in the DNS grid) and in Fig. 1(e) (in the LES grid). It can be observed that the instantaneous radiation intensity field obtained from the filtered DNS is close to the LES one. As expected, the maximum and the minimum values of $I$ are attenuated in comparison with the DNS. But it is not obvious if the instantaneous field from filtered DNS remains closer to the DNS than the LES. Moreover, comparing the fields obtained in the two grids, it is observed that the grid has an influence on the results. These observations are investigated below.

Fig. 2 displays the radiation intensity along a line of sight chosen arbitrarily from the DNS ($I_{DNS}$), from the LES ($\bar{I}_{LES}$) and from the filtered DNS ($\bar{I}_{DNS}$). The size of the filter is $\Delta = 16\delta$ and the filtering operation is three-dimensional. Three main observations can be made from this figure.

The first observation concerns the comparison between the DNS, the LES and the filtered DNS. In this particular line of sight, the profile of the radiative intensity calculated by LES ($\bar{I}_{LES}$) is closer to the DNS ($I_{DNS}$) than the filtered DNS ($\bar{I}_{DNS}$). This unexpected behavior is only observed for a few lines of sight, i.e., it is not a general trend in the system. This behavior is explained by the three-dimensional filtering effects, as shown and discussed in Section 4.1.

The second observation made from Fig. 2 is that the LES tends to underestimate the filtered radiative intensity in comparison with the filtered DNS, i.e., $\bar{I}_{LES} < \bar{I}_{DNS}$. This tendency is general and observed in the whole domain. This is explained by the influence of the SGS correlations, which are neglected in the LES, as discussed in Section 4.2.

Finally, a last observation concerns the influence of the grid. When local quantities are considered, like for instance the velocity field or the chemical composition, or in the case of thermal radiation, like the blackbody intensity, the Planck-mean absorption coefficient or the radiative emission, the coarse LES grid is well-adapted to the filtering operation and to the size of the filter. But, if non-local quantities are considered, i.e., quantities that depend on properties along the optical path, such as the radiation intensity or the radiative absorption, the change of the grid may cause additional errors in the results. In Fig. 2, the observed difference between the values of $\bar{I}_{LES}$ in the DNS grid with those obtained in the LES grid is observed at some points of the line of sight (for instance, between $\frac{s}{L} = 0.3$ and 0.6 or between $\frac{s}{L} = 0.7$ and 0.8). This difference is quite small for this particular line of sight. However, the issue about the grid influence is addressed and discussed in Section 4.3.

### 4.1. Three-dimensional filtering effects

The box filtering operation consists in averaging a given quantity in a volume of size $\Delta^3$. This is well-adapted to finite volume codes, which are the most frequently encountered in engineering applications. However, this volume averaging procedure may induce unexpected results when non-local and directional quantities are considered, such as the radiation intensity, as mentioned above.

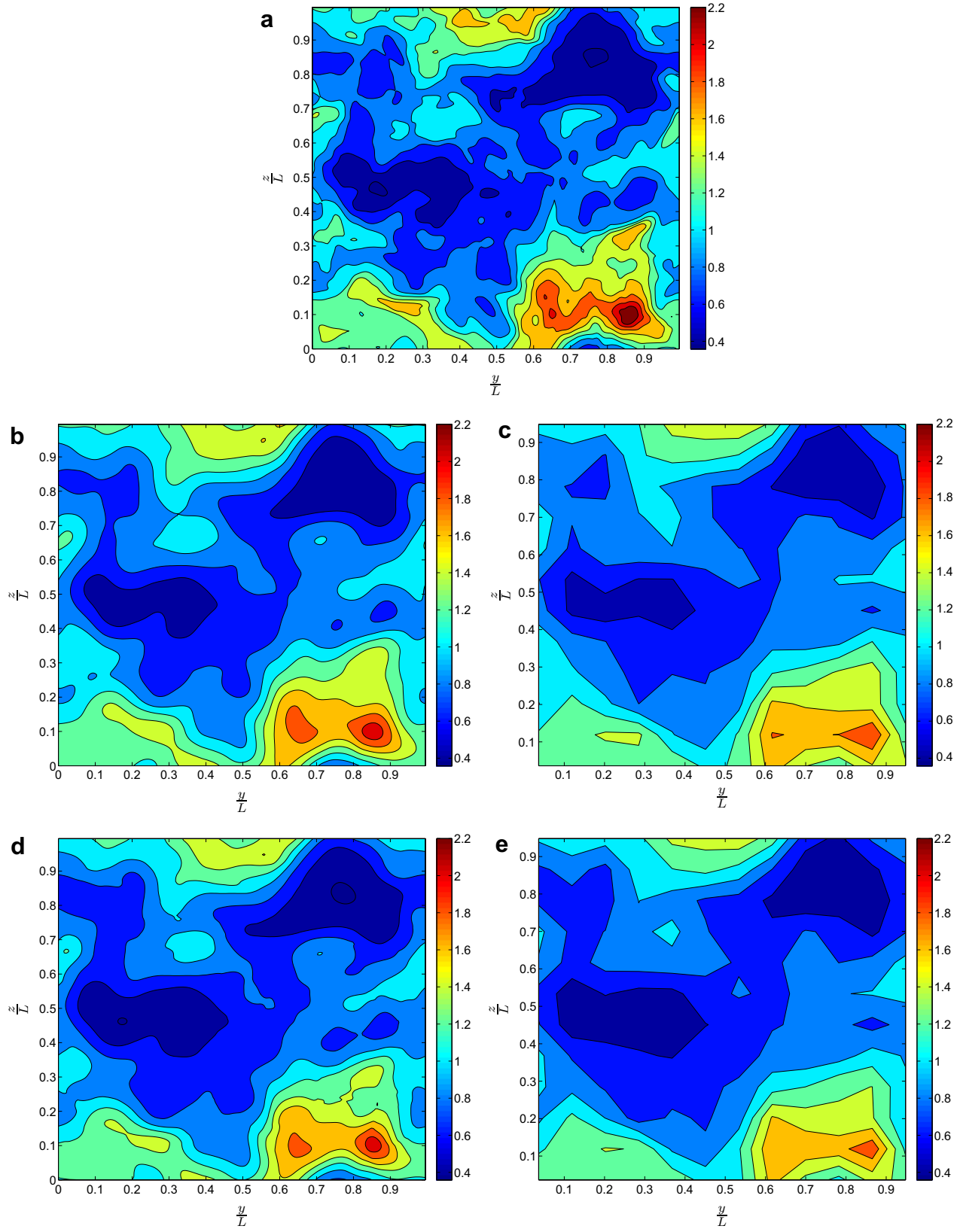


**Fig. 1.** Contours of the normalized instantaneous radiative intensity fields in a $(y, z)$ plane. (a) Displays results obtained from DNS ($I_{DNS}/\langle I_{DNS}\rangle$). (b) and (c) Display results from filtered DNS, in the DNS and in the LES grids, respectively. Calculations from LES are shown in (d) in the DNS grid, and in (e) in the LES grid. The filter size is $\Delta = 16\delta$ for (b–e).

Three-dimensional filtering has been applied in Fig. 2. In the multi-dimensional filtering operation, the filtered quantities depend on the local properties along the considered line of sight and along the neighbouring lines of sight. Fig. 3 displays a schematic of the box filtering operation in two dimensions. The neighbouring lines of sight have an influence on the values of the filtered

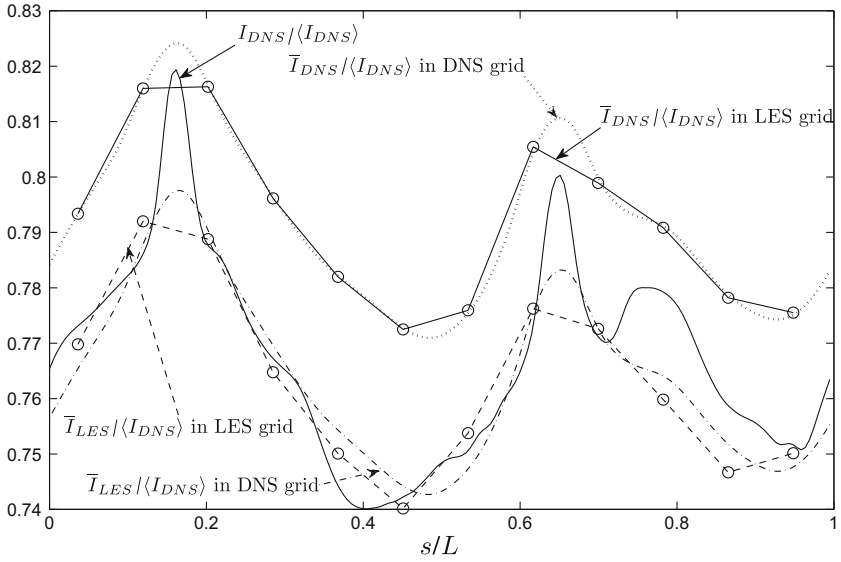


**Fig. 2.** Normalized radiative intensity profiles along a line of sight from DNS ($I_{DNS}$), LES ($\bar{I}_{LES}$) and filtered DNS ($\bar{I}_{DNS}$). The results are displayed in the DNS and in the LES grids. The filter size is $\Delta = 16\delta$.

quantities. The radiation intensity at every node of the LES grid and along the line of sight under consideration is affected by all the grid nodes within the volume defined by the filter size and centred at the corresponding LES grid node. Even though three-dimensional filtering effects are expected and may seem obvious, they are responsible for the fact that in Fig. 2, $|I_{DNS} - \bar{I}_{LES}| < |I_{DNS} - \bar{I}_{DNS}|$, which might seem surprising. However, this trend is not general, as demonstrated in Fig. 4 for another line of sight, along which $|I_{DNS} - \bar{I}_{LES}| > |I_{DNS} - \bar{I}_{DNS}|$. The different behavior of the filtered radiation intensity profiles for different lines of sight is essentially due to the three-dimensional filtering effects, as shown in Fig. 5. In this figure, the radiation intensity profiles are displayed along the same line of sight considered in Fig. 2, except that the filtering operation is now one-dimensional, i.e., it is applied only along the considered line of sight. In this case, $|I_{DNS} - \bar{I}_{LES}| > |I_{DNS} - \bar{I}_{DNS}|$, showing that the different trend in Fig. 2 is indeed a consequence of the three-dimensional filtering.

All the results reported in the following sections were obtained using a three-dimensional filter, since this is predicted in LES of the Navier-stokes equations.

### 4.2. Influence of the subgrid-scale correlations on the thermal radiation

In the present LES, all the subgrid-scale correlations have been neglected, namely the temperature self-correlation, i.e., $\overline{T^4} \simeq \overline{T}^4$, the absorption coefficient-blackbody intensity correlation (analogous to the absorption coefficient-temperature correlation), i.e., $\overline{\kappa_\nu I_{b\nu}} \simeq \bar{\kappa}_\nu \bar{I}_{b\nu}$ and the absorption coefficient-radiation intensity correlation, i.e., $\overline{\kappa_\nu I_\nu} \simeq \bar{\kappa}_\nu \bar{I}_\nu$. The absorption coefficient self-correlation is smaller than the others, i.e., $\bar{\kappa}_P \simeq \kappa_P(\overline{T}, \overline{X}_{CO_2})$, and will be ignored in the present analysis. The comparison of the LES with the filtered DNS may give some indications about the relevance of these subgrid-scale correlations on the estimated thermal radiation.

Tables 2 and 3 display comparisons of mean values obtained from LES and from filtered DNS. The angle brackets $\langle\rangle$ represent time-averaged quantities. In the present case, where statistically steady homogeneous isotropic turbulence is considered, the time-averaged and the space-averaged quantities are equal. Thus, the mean values presented in these tables are estimated from a space-averaging of the quantities over all the computational

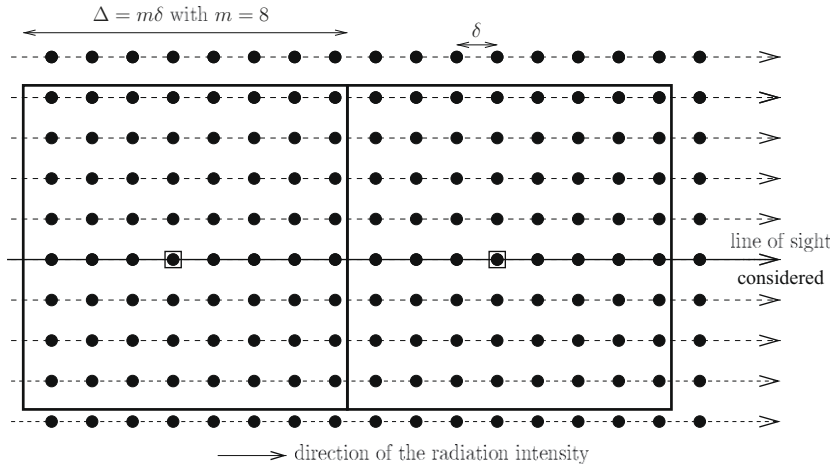


**Fig. 3.** Schematic representing the box filtering operation (in two dimensions). The LES grid nodes are represented by squares whereas the DNS grid nodes are represented by circles.

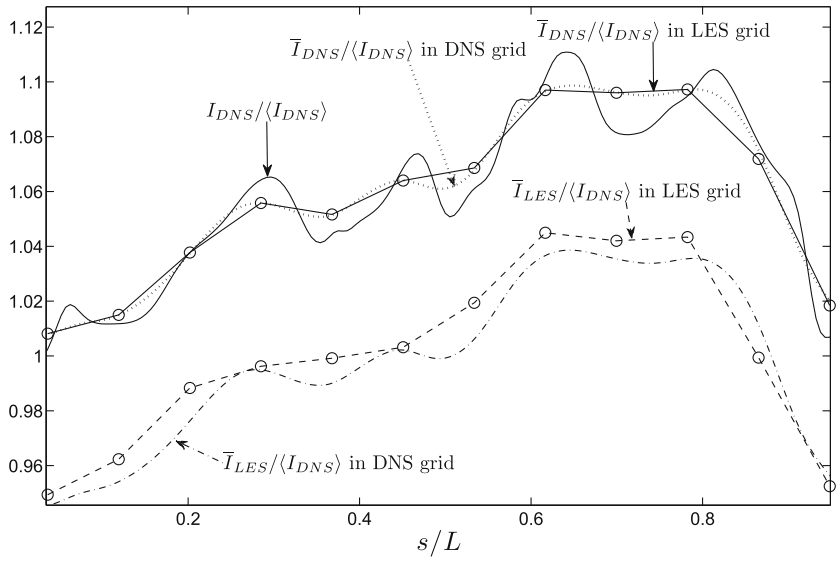


**Fig. 4.** Normalized radiative intensity profiles along a different line of sight, from DNS ($I_{DNS}$), LES ($\overline{I}_{LES}$) and filtered DNS ($\overline{I}_{DNS}$). The results are displayed in the DNS and in the LES grids. The filter size is $\Delta = 16\delta$.

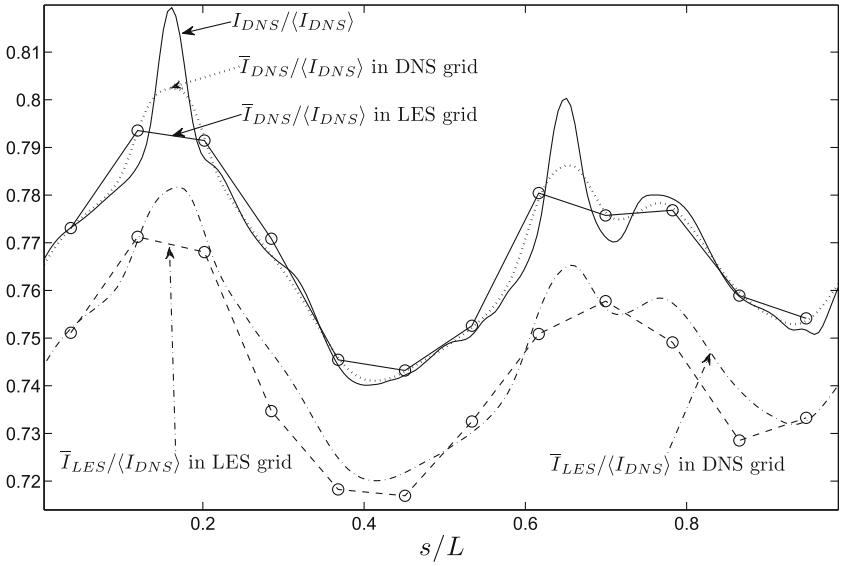


**Fig. 5.** Normalized radiative intensity profiles along a line of sight (same as in Fig. 2) from DNS ($I_{DNS}$), LES ($\overline{I}_{LES}$) and filtered DNS ($\overline{I}_{DNS}$). The filtering operation is one-dimensional. The results are displayed in the DNS and in the LES grids. The filter size is $\Delta = 16\delta$.

domain at a given instant. All the grid nodes of the LES mesh have been used to compute the mean values.

Table 2 presents the ratios of the mean radiation intensity calculated by LES to the mean radiation intensity obtained from filtered DNS, for various filter sizes. The same ratio is given for the blackbody radiative intensity. The mean blackbody intensity ratio allows to evaluate the influence of the subgrid-scale temperature self-correlation on the results, recalling that $\langle I_b(\overline{T})\rangle/\langle\overline{I}_{b,DNS}\rangle = \langle\overline{T}^4\rangle/\langle\overline{T^4}\rangle$. This ratio is clearly less than 1, showing that the subgrid-scale temperature self-correlation tends to increase the filtered blackbody intensity. In the case of a box filter, where a filtered quantity is equal to the arithmetic mean of the considered quantity over the points within the volume defined by the filter width, it is easy to demonstrate that $\overline{T}^4/\overline{T^4}$ is always less than or equal to one, as shown in [11]. The effect of the non-resolved scales of the temperature field on the resolved blackbody intensity be-

**Table 2**
Ratio of mean values obtained from LES to mean values obtained from filtered DNS for the radiation intensity and the blackbody intensity.

| $\Delta/\delta$ | 2 | 4 | 8 | 16 | 32 |
|---|---|---|---|---|---|
| $\langle I_b(\overline{T})\rangle/\langle\overline{I}_{b,DNS}\rangle$ | 0.998 | 0.991 | 0.974 | 0.939 | 0.881 |
| $\langle\overline{I}_{LES}\rangle/\langle\overline{I}_{DNS}\rangle$ | 0.995 | 0.993 | 0.978 | 0.949 | 0.906 |

**Table 3**
Ratio of mean values obtained from LES to mean values obtained from filtered DNS for the radiative emission and absorption.

| $\Delta/\delta$ | 2 | 4 | 8 | 16 | 32 |
|---|---|---|---|---|---|
| $\langle\overline{\kappa_P}\overline{I}_{bDNS}\rangle/\langle\overline{\kappa_P I_{bDNS}}\rangle$ | 1.002 | 1.009 | 1.029 | 1.069 | 1.136 |
| $\langle\kappa_P(\overline{T},\overline{X}_{CO_2})I_b(\overline{T})\rangle/\langle\overline{\kappa_P I_{bDNS}}\rangle$ | 1 | 0.998 | 0.995 | 0.987 | 0.975 |
| $\langle\overline{\kappa_G}\overline{I}_{DNS}\rangle/\langle\overline{\kappa_G I}_{DNS}\rangle$ | 1 | 1 | 1.001 | 1.004 | 1.010 |

come apparent through the following expansion of the filtered blackbody intensity,

$$\bar{I}_{b,DNS} = \frac{\sigma\overline{T^4}}{\pi} \simeq \frac{\sigma\overline{T}^4}{\pi}\left(1 + \frac{6\overline{T''^2}}{\overline{T}^2} + \frac{4\overline{T''^3}}{\overline{T}^3} + \frac{\overline{T''^4}}{\overline{T}^4}\right) \tag{17}$$

where it is assumed that $\overline{\overline{T}} = 0$ and $\overline{T''} = 0$ (which is exact for a cut-off filter), and the temperature is decomposed as the sum of a resolved ($\overline{T}$) and a subgrid-scale component ($T''$) [10]. The term that involves the third power of the temperature is generally negligible, while the second and the fourth terms on the right hand side of Eq. (17) are both positive. Therefore, the subgrid-scale temperature in the LES tends to increase the resolved blackbody intensity. For $\Delta = 16\delta$, a significant increase (of about 6%) is observed.

Concerning the radiative intensity, the results in Table 2 confirm the second observation made previously from Fig. 2, i.e., $\langle\bar{I}_{LES}\rangle/\langle\bar{I}_{DNS}\rangle < 1$ which means that the calculations from LES tend to underestimate the radiation intensity. When $\Delta/\delta = 2, 4$ and 8, the mean radiation intensity estimated by LES is very close to the filtered DNS. But when $\Delta/\delta = 16$, the difference between the two filtered radiative intensities exceeds 5%. It should be noted that it is not possible to identify the effect of a particular SGS correlation from this ratio. In fact, according to the filtered RTE solved by the LES without accounting for the SGS contributions (cf Eq. 6), it is the combined effect of all the SGS correlations that is highlighted in $\langle\bar{I}_{LES}\rangle/\langle\bar{I}_{DNS}\rangle$.

In Table 3, results concerning the radiative emission and the radiative absorption are presented. It is observed that $\langle\bar{\kappa}_P\bar{I}_{bDNS}\rangle/\langle\overline{\kappa_P I_{bDNS}}\rangle$ is greater than 1. Since $\langle\overline{\kappa_P I_{bDNS}}\rangle = \langle\bar{\kappa}_P\bar{I}_{bDNS}\rangle + \langle(\overline{\kappa_P I_{bDNS}} - \bar{\kappa}_P\bar{I}_{bDNS})\rangle$, the term into parenthesis, which accounts for the time-averaged SGS absorption coefficient-temperature correlation, is negative and contributes to decrease the time-averaged filtered emission $\langle\overline{\kappa_P I_{bDNS}}\rangle$. On the other hand, $\langle\kappa_P(\overline{T},\overline{X}_{CO_2})I_b(\overline{T})\rangle/\langle\overline{\kappa_P I_{bDNS}}\rangle$ is lower than 1. Therefore, the time-averaged SGS correlations in the emission term, which are fully ignored in the product $\langle\kappa_P(\overline{T},\overline{X}_{CO_2})I_b(\overline{T})\rangle$, are positive, *i.e.*, $\langle(\overline{\kappa_P I_{bDNS}} - \kappa_P(\overline{T},\overline{X}_{CO_2})I_b(\overline{T}))\rangle > 0$. The SGS temperature self-correlation and the SGS absorption coefficient self-correlation are both ignored when $\langle\kappa_P(\overline{T},\overline{X}_{CO_2})I_b(\overline{T})\rangle$ is considered instead of $\langle\bar{\kappa}_P\bar{I}_b\rangle$. Since the contribution of the SGS absorption coefficient self-correlation is marginal, it may be concluded that the SGS temperature self-correlation is responsible for the sign change of the SGS correlations. It can be further concluded that the SGS absorption coefficient-temperature correlation and the SGS temperature self-correlation have opposite signs. The opposite effect of the SGS correlations and the improved prediction of $\langle\overline{\kappa_P I_b}\rangle$ obtained when all the SGS correlations are ignored (the ratio on the second row is closer to unity than the ratio on the first row of Table 3) imply that it is better to neglect all SGS correlations, instead of modelling only one in LES. These results confirm the a-priori study of Poitou et al. [10] where the filtered emission estimated with a SGS model only for the temperature self-correlation yields worst results than the filtered emission estimated without any SGS model.

Regarding now the filtered radiative absorption, Table 3 shows that the ratio $\langle\bar{\kappa}_G\bar{I}\rangle/\langle\overline{\kappa_G I}\rangle$ is higher than 1. Therefore, the absorption coefficient-radiation intensity SGS correlation tends to decrease the filtered radiative absorption, but its influence on the radiative absorption seems to be weaker than the influence of the other correlations.

*Influence of the variance and of the mean temperature on the SGS correlations*. Fig. 6 displays the influence of the temperature variance on the filtered radiative intensity. The mean temperature is fixed at 1500 K. The ratio $\langle\bar{I}_{LES}\rangle/\langle\bar{I}_{DNS}\rangle$ decreases with the increase of $\langle T'^2\rangle$, as expected. This figure confirms the a-priori results presented in [17], i.e., the temperature turbulence intensity has a strong influence on the importance of the subgrid-scale correlation in LES of radiative heat transfer. When the temperature turbulence intensity exceeds 20%, the subgrid-scale fluctuations become important, *e.g.*, when $\frac{\sqrt{\langle T'^2\rangle}}{\langle T\rangle} = 30\%$ and $\Delta = 16\delta$, the difference between $\bar{I}_{LES}$ and $\bar{I}_{DNS}$ reaches 10%.

Fig. 7 shows the influence of the mean temperature $\langle T\rangle$ on the radiative intensity. These results were obtained for a constant temperature turbulence intensity $\sqrt{\langle T'^2\rangle}/\langle T\rangle$ fixed at 20%. The ratio $\langle\bar{I}_{LES}\rangle/\langle\bar{I}_{DNS}\rangle$ increases with $\langle T\rangle$, which means that the combined effect of all the subgrid-scale correlations tends to decrease with the increase of the mean temperature. This supports the assumption which consists in neglecting the TRI in LES, since TRI effects seem to be more significant in systems where the mean temperature is relatively low, i.e., when the radiative heat transfer is less important.

The influence of the mean temperature on the filtered emission and absorption, is displayed in Figs. 8 and 9, respectively, for various filter sizes, and for a constant $\sqrt{\langle T'^2\rangle}/\langle T\rangle$ equal to 20%. Fig. 8 shows that the influence of the absorption coefficient-temperature SGS correlation is more important for larger values of $\langle T\rangle$, i.e., the ratio $\langle\bar{\kappa}_P\bar{I}_{bDNS}\rangle/\langle\overline{\kappa_P I_{bDNS}}\rangle$ increases with $\langle T\rangle$. Moreover, the ratio $\langle\kappa_P(\overline{T},\overline{X}_{CO_2})I_b(\overline{T})\rangle/\langle\overline{\kappa_P I_{bDNS}}\rangle$, which is lower than 1, increases and

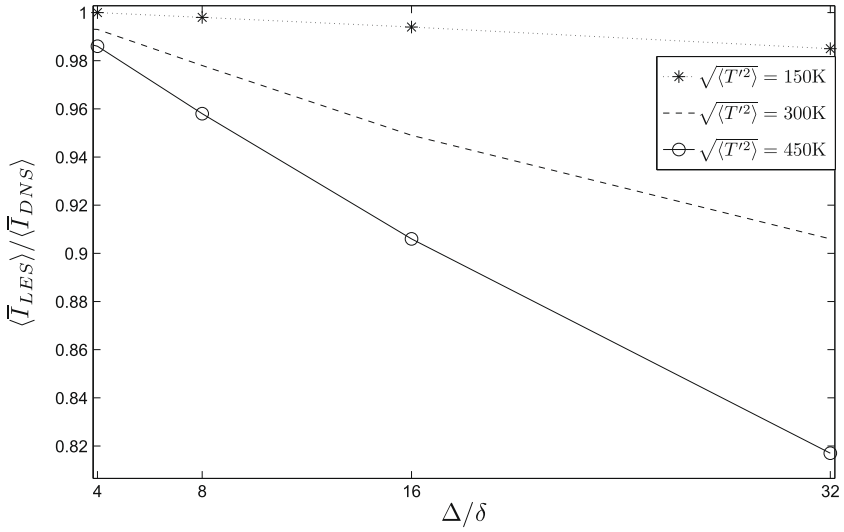


**Fig. 6.** Influence of the temperature variance on the ratio $\langle\bar{I}_{LES}\rangle/\langle\bar{I}_{DNS}\rangle$. The mean temperature $\langle T\rangle$ is fixed at 1500 K.

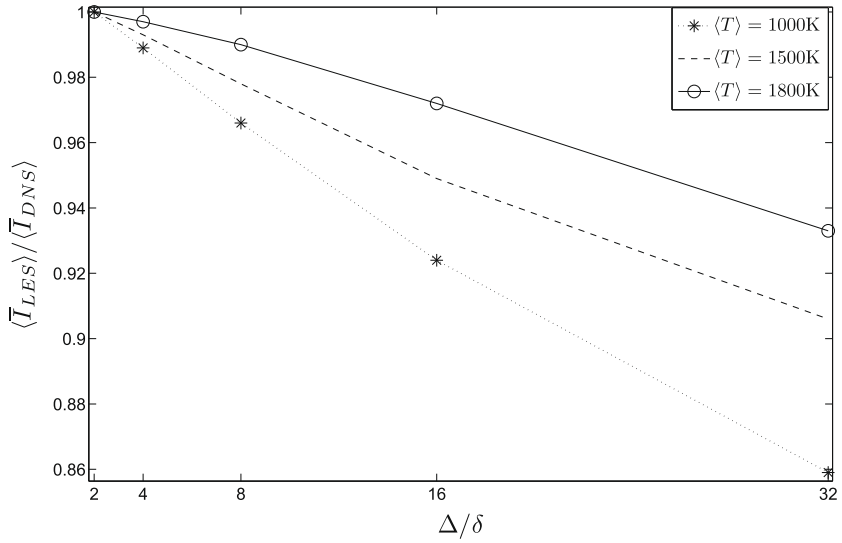


**Fig. 7.** Influence of the mean temperature on the ratio $\langle \bar{I}_{LES}\rangle/\langle \bar{I}_{DNS}\rangle$. The temperature turbulence intensity $\frac{\sqrt{\langle T'^2\rangle}}{\langle T\rangle}$ is fixed at 20%.

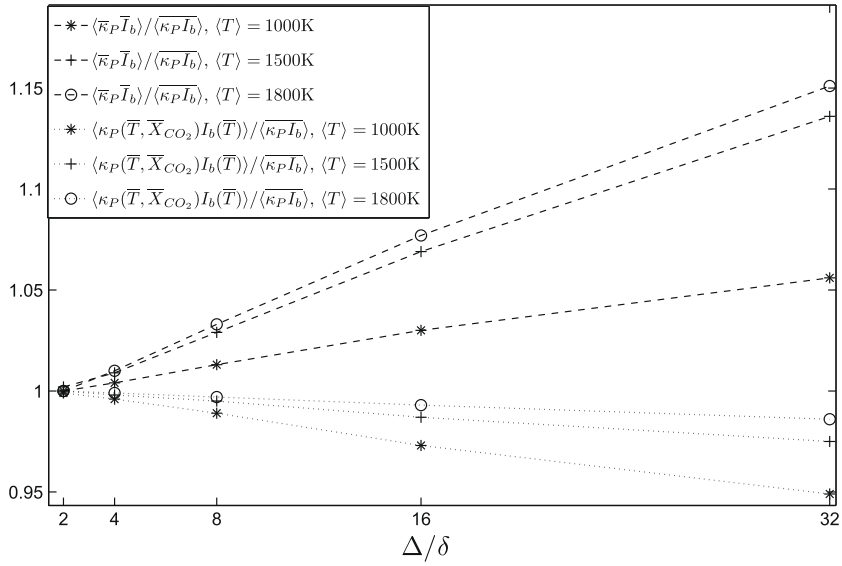


**Fig. 8.** Influence of the mean temperature on the ratios $\langle \kappa_P(\bar{T}, \bar{X}_{CO_2}) I_b(\bar{T})\rangle / \langle \overline{\kappa_P I_b}\rangle$ and $\langle \bar{\kappa}_P \bar{I}_b\rangle / \langle \overline{\kappa_P I_b}\rangle$. The temperature turbulence intensity $\frac{\sqrt{\langle T'^2\rangle}}{\langle T\rangle}$ is fixed at 20%.

gets closer to 1 when $\langle T\rangle$ increases. This reveals that the SGS absorption coefficient-temperature correlation tends to compensate the temperature self-correlation (constant) as the time-averaged temperature increases, since these correlations have opposite signs on average, as formerly discussed. Therefore, the predictions obtained by simply ignoring all the SGS correlations are more accurate for high value of $\langle T\rangle$, *e.g.*, when $\langle T\rangle$ is equal to 1800K. This confirms that the TRI effects on the filtered radiative emission are more important at low mean temperature, and therefore the subgrid-scale correlations are more important at low-temperature, when the radiative heat transfer is lower. In Fig. 9, the ratio $\langle \bar{\kappa}_G \bar{I}_{DNS}\rangle / \langle \overline{\kappa_G I}_{DNS}\rangle$ increases with $\langle T\rangle$, but remains close to 1. For instance, when $\Delta = 2\delta$ and $\Delta = 4\delta$, the influence of the subgrid-scale on the radiative absorption is too small to be characterized by $\langle \bar{\kappa}_G \bar{I}_{DNS}\rangle / \langle \overline{\kappa_G I}_{DNS}\rangle$, which is equal to 1 in both cases. The correlation between the absorption coefficient and the radiation intensity is less significant than the other SGS correlations. If $\langle T\rangle = 1000$ K, this correlation tends to increase the filtered radiative absorption, i.e., $\langle \bar{\kappa}_G \bar{I}_{DNS}\rangle / \langle \overline{\kappa_G I}_{DNS}\rangle < 1$, while if $\langle T\rangle = 1500$ K or 1800 K, the ratio is greater than 1. However, this influence remains small, which confirms previous results in [11,17], where it is suggested that the optically thin fluctuation approximation usually assumed in RANS applications should be appropriate to LES.

### 4.3. Influence of the grid on the radiation intensity

In Fig. 2, it was observed that the grid has an influence, although quite small, on the radiation intensity. It can be seen that in the common nodes of the LES and the DNS grids, the radiation intensity from filtered DNS ($\bar{I}_{DNS}$) remains equal in both grids, as expected. But, the LES results exhibit a difference in the LES grid and in the DNS grid. This difference, observed only for non-local quantities, such as the radiation intensity or the radiative absorption, highlights the influence of the grid.

The normalized difference $(\bar{I}_{DNS} - \bar{I}_{LES})/\langle I_{DNS}\rangle$ between the radiation intensity from filtered DNS and from LES, in both LES and DNS grids, is shown in Fig. 10. The filter size is $\Delta = 16\delta$, and the line of sight is the same as in Fig. 2. It is shown that the coarser grid affects

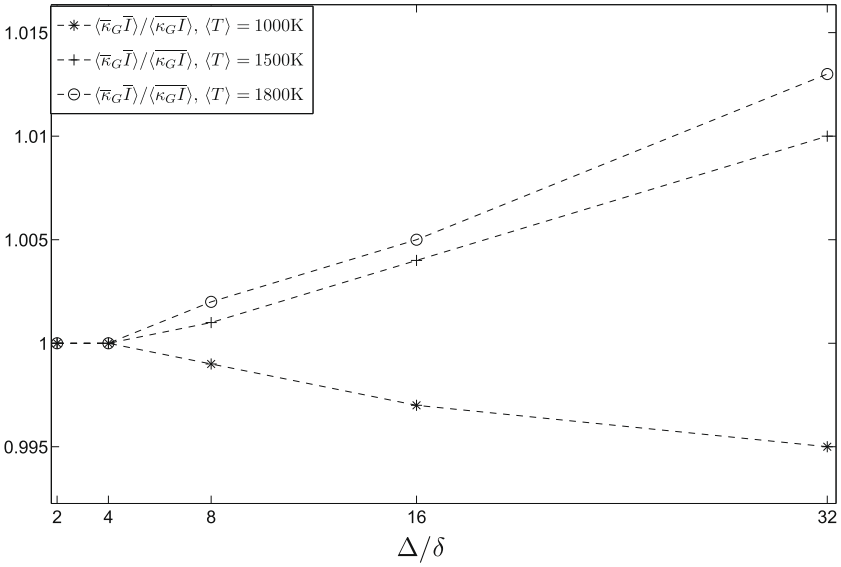


**Fig. 9.** Influence of the mean temperature on the ratio $\langle\bar{\kappa}_G\bar{I}\rangle/\langle\overline{\kappa_G I}\rangle$. The temperature turbulence intensity $\frac{\sqrt{\langle T'^2\rangle}}{\langle T\rangle}$ is fixed at 20%.

$\bar{I}_{LES}$ at some points, like for instance when $s/L \in [0.3, 0.5]$ or $s/L \in [0.8, 0.9]$. The difference $|\bar{I}_{DNS} - \bar{I}_{LES}|$ is higher in the LES grid than in the DNS grid. The radiation intensity is a non-local quantity and consequently the error due to the lack of subgrid-scale modelling spreads and changes along an optical path. Moreover, due to the three-dimensional effect, the influence of the neighbouring lines of sight increases this error at some points and decreases it at others.

However, the overall influence of the grid is quite small. The computations show that $\langle\bar{I}_{DNS} - \bar{I}_{LES}\rangle_{DNSgrid}/\langle\bar{I}_{DNS} - \bar{I}_{LES}\rangle_{LESgrid} = 0.997$ for $\Delta = 16\delta$, which is much closer to 1 than the ratio $\langle\bar{I}_{LES}\rangle/\langle\bar{I}_{DNS}\rangle$ (equal to 0.946 in the same conditions), which describes the SGS correlation effects. Similar trends were found for other lines of sight. Therefore, the influence of the grid may be neglected in future TRI modelling.

## 5. Conclusion

The turbulence–radiation interaction in the LES framework was studied by solving the filtered RTE without any SGS model and by comparing the predictions with filtered DNS results from statistically stationary (forced) homogeneous isotropic turbulence. Previous LES of radiating flows neglected the influence of the SGS on the radiative heat transfer. The consequences of this assumption were analysed in order to shed some light on future SGS modelling of thermal radiation.

The SGS correlation effects have been studied. The temperature self-correlation and the absorption coefficient-temperature correlation were evaluated. The temperature self-correlation, which increases the filtered radiative emission, is stronger than the absorption coefficient-temperature correlation, which decreases the filtered emission. This opposite effect implies that it should be better to neglect both correlations instead of modelling only one. The SGS correlation between the radiation intensity and the absorption coefficient is weaker.

The study of the influence of the mean and variance of the temperature has shown that the TRI effects are more significant when temperature fluctuations are higher and low-temperature systems are considered. This supports the conclusion drawn in [11], which states that TRI in LES is less significant than in the RANS context. In fact, the radiative heat transfer is lower in low-temperature

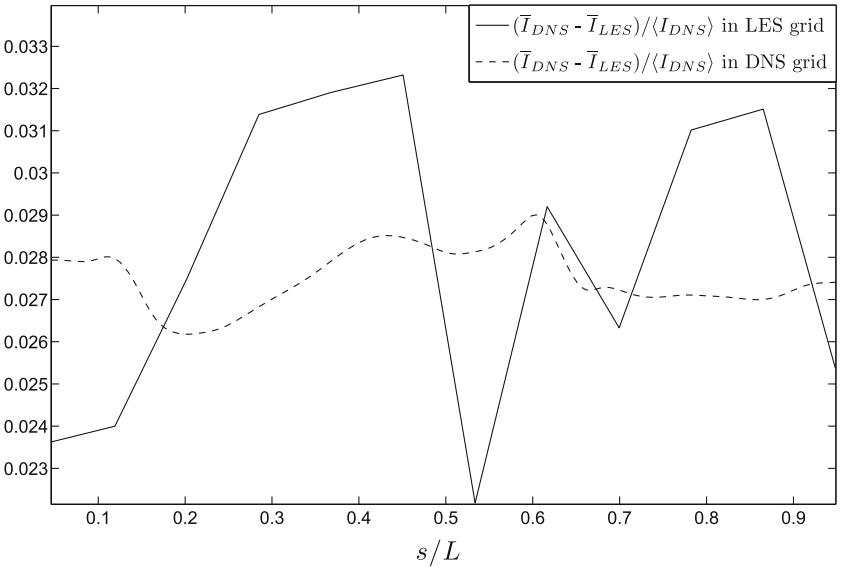


**Fig. 10.** Difference between filtered DNS and LES for the radiation intensity along a line of sight. The size of the filter is $\Delta = 16\delta$.

systems and consequently the need for subgrid-scale modelling of TRI is lower. However, the combined effect of all the SGS correlations leads to an error on the filtered radiation intensity higher than 5% when the mean temperature is equal to 1500 K, the temperature turbulence intensity is 20% and when the implicit filter is located at the inertial range of the kinetic energy spectrum, which is typical of engineering applications. These physical conditions can be encountered in many engineering systems, with high temperature fluctuations, which imply a bigger influence of the TRI. In these cases, subgrid-scale models should be developed.

The influence of the three-dimensional filtering has also been studied. The multi-dimensional box filtering operation of a non-local radiation quantity (such as the radiation intensity or the radiative absorption) implies that this quantity depends not only on the physical properties along the line of sight, but also on the physical properties along the neighbouring lines of sight, which are located in the same volume defined by the box filter size. This may significantly modify the local radiation intensity. However, no general tendency is observed, suggesting that this effect can be ignored in future SGS modelling. The influence of the grid on the non-local quantities has also been quantified, and remains weaker than the SGS correlation effects.

The analysis proposed in the present study is based on an idealised physical configuration, i.e. statistically steady forced homogeneous isotropic turbulence, in order to clarify the analysis and give fundamental insight on the relevance of the TRI in LES framework. Therefore, care should be taken in extrapolation of the present conclusions to practical reactive flows. The extension of this analysis to more realistic cases will be the purpose of future work, as well as the development of efficient SGS models for thermal radiation, with the objective of including radiative heat transfer calculations in LES of reactive flows.

## Acknowledgements

This work was developed within the framework of project PPCDT/EME/59879/2004, which is financially supported by FCT-Fundação para a Ciência e a Tecnologia, project No. 3599. M. Roger acknowledges the FCT-Fundação para a Ciência e a Tecnologia for the postdoc fellowship SFRH/BPD/34014/2006.

## References

[1] P.J. Coelho, Numerical simulation of the interaction between turbulence and radiation in reactive flows, Prog. Energy Combust. Sci. 33 (4) (2007) 311–384.
[2] P.J. Coelho, Detailed numerical simulation of radiative transfer in a nonluminous turbulent jet diffusion flame, Combust. Flame 136 (4) (2004) 481–492.
[3] S. Mazumder, M.F. Modest, A probability density function approach to modeling turbulence–radiation interactions in nonluminous flames, Int. J. Heat Mass Transfer 42 (6) (1999) 971–991.
[4] L.H. Liu, X. Xu, Y.L. Chen, On the shapes of the presumed probability density function for the modeling of turbulence–radiation interactions, J. Quant. Spectrosc. Radiat. Transfer 87 (3–4) (2004) 311–323.
[5] Y. Wu, D.C. Haworth, M.F. Modest, B. Cuenot, Direct numerical simulation of turbulence/radiation interaction im premixed combustion systems, Proc. Combust. Instit. 30 (1) (2005) 639–646.
[6] K.V. Deshmukh, D. C Haworth, M.F. Modest, Direct numerical simulation of turbulence–radiation interactions in homogeneous nonpremixed combustion systems, Proc. Combust. Instit. 31 (1) (2007) 1641–1648.
[7] K.V. Deshmukh, M.F. Modest, D. C Haworth, Direct numerical simulation of turbulence–radiation interactions in a statistically one-dimensional nonpremixed system, J. Quant. Spectrosc. Radiat. Transfer 109 (14) (2008) 2391–2400.
[8] S.B. Pope, Turbulent Flows, Cambridge University Press, 2000.
[9] J. Janicka, A. Sadiki, Large eddy simulation of turbulent combustion systems, Proc. Combust. Instit. 30 (1) (2005) 537–547.
[10] D. Poitou, M. El Hafi, B. Cuenot, Diagnosis of turbulence radiation interaction in turbulent flames and implications for modeling in large eddy simulation, Turkish J. Eng. Environ. Sci. 31 (6) (2007) 371–381.
[11] P.J. Coelho, Approximate solutions of the filtered radiative transfer equation in large eddy simulations of turbulent reactive flows, Combust. Flame 156 (5) (2009) 1099–1110.
[12] P.E. Desjardin, S.H. Frankel, Two-dimensional large eddy simulation of soot formation in the near-field of a strongly radiating non-premixed acetylene-air turbulent jet flame, Combust. Flame 119 (1–2) (1999) 121–132.
[13] D.C. Haworth, V. Singh, A. Gupta, M.F. Modest, Large eddy simulation of turbulent flows with thermal radiation and turbulence/radiation interaction, in: 58th Annu. Meeting of the American Physical Society Division of Fluid Dynamics, 2005.
[14] W.P. Jones, M.C. Paul, Combination of DOM with LES in a gas turbine combustor, Int. J. Eng. Sci. 43 (5-6) (2005) 379–397.
[15] R. Gonçalves dos Santos, M. Lecanu, S. Ducruix, O. Gicquel, E. Diacona, D. Veynante, Coupled large eddy simulations of turbulent combustion and radiative heat transfer, Combust. Flame 152 (3) (2008) 387–400.
[16] M. Roger, P.J. Coelho, C.B. da Silva, Analysis of the relevance of the filtered radiative transfer equation terms for large eddy simulation of turbulence–radiation interaction, in: Proceedings of CHT-08, ICHMT Int. Symposium on Advances in Computational Heat Transfer, May 11–16, 2008, Marrakech, Morocco, 2008.
[17] Maxime Roger, Carlos B. da Silva, Pedro J. Coelho, Analysis of the turbulence–radiation interactions for large eddy simulation of turbulent flows, Int. J. Heat Mass Transfer 52 (9-10) (2009) 2243–2254.
[18] M.F. Modest, Radiative Heat Transfer, McGraw-Hill, New-York, 2003.
[19] K. Alvelius, Random forcing of three-dimensional homogeneous turbulence, Phys. Fluids 11 (7) (1999) 1880–1889.
[20] C.B. da Silva, I. Malico, P.J. Coelho, Radiation statistics in homogeneous isotropic turbulence, New J. Phys. 11 (2009) 093001.
[21] C.B. da Silva, J.C.F. Pereira, Analysis of the gradient-diffusion hypothesis in large-eddy simulations based on transport equations, Phys. Fluids 19 (2007) 035106.
[22] R. Rogallo, P. Moin, Numerical simulation of turbulent flows, Annu. Review Fluid Mech. 16 (1984) 99–137.
[23] R.M. Goody, R. West, L. Chen, D. Crisp, The correlated-k method for radiation calculations in non-homogeneous atmospheres, J. Quant. Spectrosc. Radiat. Transfer 42 (6) (1989) 539–550.
[24] A. Soufiani, J. Taine, High temperature gas radiative property parameters of statistical narrow-band model for $H_2O$, $CO_2$ and CO, and correlated-K model for $H_2O$ and $CO_2$, Int. J. Heat Mass Transfer 40 (4) (1997) 987–991.